



GE Nuclear Energy

---

TECHNICAL MODIFICATIONS SERVICES  
GE-NE-523-B13-01805-105, Rev. 2  
October 1996

## **EVALUATION OF INDICATIONS AT THE COLLAR TO SHROUD WELD OF VERMONT YANKEE ANNULUS CORE SPRAY PIPING**

Prepared for

Yankee Atomic Electric Co.  
580 Main Street  
Bolton, MA 01740-1398

Prepared by

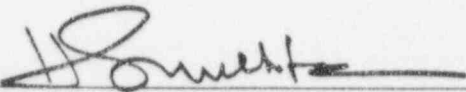
GE Nuclear Energy  
175 Curtner Avenue  
San Jose, CA 95125

9610170163 961009  
PDR ADOCK 05000271  
Q PDR

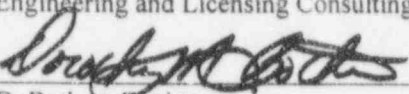
**EVALUATION OF INDICATIONS AT  
THE COLLAR TO SHROUD WELD OF  
VERMONT YANKEE ANNULUS CORE SPRAY PIPING**

October 1996

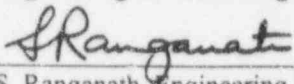
Prepared by:

  
H.S. Mehta, Principal Engineer  
Engineering and Licensing Consulting Services

Prepared by:

  
D. Bothne, Engineer  
Engineering and Licensing Consulting Services

Verified by:

  
S. Ranganath, Engineering Fellow  
Office of Chief Technologist

Approved by:

  
B. A. McAllister, RIM Project Manager  
Nuclear Services Department

TABLE OF CONTENTS

1. INTRODUCTION AND BACKGROUND	3
2. CRACK GROWTH RATE CONSIDERATIONS	3
3. STRUCTURAL MARGIN EVALUATION	4
4. INSTALLATION TOLERANCES	6
5. FIV EVALUATION ASSUMING COMPLETE FAILURE OF COLLAR WELD	7
6. EVALUATION ASSUMING INDICATIONS IN SHROUD	7
7. SUMMARY & CONCLUSIONS	8
8. REFERENCES	9

## 1. INTRODUCTION AND BACKGROUND

The annulus core spray piping is attached to the shroud via a collar. The collar to shroud weld is designated as weld P8b in the BWRVIP Core Spray Line I&E Guidelines document [1]. Figure 1 from Reference 1 shows a schematic of this weld. The collar is not associated with the core spray injection flow. Its purpose is to prevent leakage from the inside to the outside of the core shroud at the location where the core spray piping enters the shroud. In addition, it provides the attachment of the core spray piping to the shroud. This adds stiffness to the piping and helps to assure that the piping will not be subject to flow induced vibration (FIV).

During the ultrasonic examination of this weld at 193° azimuth at Vermont Yankee (VY) plant, six circumferential indications associated with IGSCC/IASCC were recorded. Figure 2 shows the specific parameters for these indications. The UT data show the indications appear to be located in the HAZ of the core shroud itself, rather than in the thermal sleeve collar. This in itself is not a unique finding, in that two other plants have detected indications in the shroud at locations where brackets have been attached to the shroud by fillet welds. The subject core spray collar is welded to the outside of the shroud with a somewhat similar weld.

A second collar (at vessel azimuth 13°) had a smaller indication. This evaluation is applicable to both collars.

This report describes the results of structural evaluations considering two limiting assumptions: (1) the indications are located in the collar, and (2) the indications are located in the shroud. The first assumption is more limiting since cracking in the sleeve (unlike that in the shroud wall) is likely to be through thickness.

## 2. CRACK GROWTH RATE CONSIDERATIONS

The inspection results indicate that the indications are of IGSCC origin. Therefore, a key input in the structural margin evaluation in the presence of these indications is the crack growth rate. The BWRVIP Guidelines document [1] recommends a conservative crack growth rate of  $5 \times 10^{-5}$  in/hr.



The preceding crack growth is expected to be conservative for this application based on several reasons. First, the reactor water conductivity at the VY plant has been better than the U.S. BWR Fleet average. The coolant conductivity at the VY plant has averaged 0.11  $\mu\text{S/cm}$  over the last three cycles as compared with a conductivity of  $\sim 0.3 \mu\text{S/cm}$  during the first five cycles of operation. Figure 3 shows the crack growth rate predicted by the GE PLEDGE code as a function of water conductivity. An improvement of better than a factor of 2 is seen as the conductivity decreases from 0.3  $\mu\text{S/cm}$  to 0.1  $\mu\text{S/cm}$ . The BWR normal water chemistry guidelines typically set action level 1 at conductivity greater than 0.3  $\mu\text{S/cm}$ . Thus, if one were to assume that the  $5 \times 10^{-5}$  in/hr growth rate is applicable for a reactor water conductivity of 0.3  $\mu\text{S/cm}$ , the predicted crack growth rate for VY is expected to be  $2.5 \times 10^{-5}$  in/hr or less.

Another approach to calculate the average crack growth rate is to base it on the largest indication length divided by the operating hours since the assumed initiation. The largest indication length in Table 1 is 4.52 inch. The VY plant has been in commercial operation since 1972. The field experience shows that cracking in the core spray piping or spargers has been seen as early as 8 years of commercial operation. If it is assumed that the initiation occurred after approx. 12 years of commercial operation, then the crack growth period is approximately 96000 hours. This implies a crack growth rate of  $(4.52/[2 \times 96000])$  or  $2.4 \times 10^{-5}$  in/hr. The factor of 2 in the preceding calculation accounts for the fact that the crack growth at each end of the indication.

Based on the preceding discussion it is concluded that the crack growth rate of  $5 \times 10^{-5}$  in/hr used in this evaluation is conservative.

### 3. STRUCTURAL MARGIN EVALUATION

This Section describes the structural margin evaluation assuming the indications to be on the collar side of the weld. The second column from right hand side in Table 1 shows the as-found ligament lengths between the six circumferential indications. The values range from 0.50 in. to 1.81 in. For a conservative crack growth rate of  $5.0 \times 10^{-5}$  in/hr, the calculated values of remaining ligament lengths at the end of one cycle of operation are shown in the last right hand column of Table 1. A review of the last column shows the remaining ligament to be 0.61 inch. With this calculated remaining ligament length, this weld would not have the moment load carrying capability. Therefore, it was assumed that this ligament is capable of only supporting an axial force. The ligament area is  $(0.61 \times 0.1565)$  or  $0.095 \text{ in}^2$ . The axial force carrying capability of this ligament was calculated as

4816 lbs assuming a material flow stress of 50700 psi ( $S_m = 16900$  psi @ 550°F and flow stress =  $3S_m$ ).

The next step in the evaluation process was to determine the maximum value of the axial force at the collar weld location. A flaw tolerance evaluation of the core spray line has been documented in Reference 2 (included as Appendix to this report). Since the collar weld is now assumed to have no moment carrying capability, the finite element model consisting of one loop of the VY core spray piping system (see Figure 4), developed to determine the stresses from various design loads was modified to reflect hinged boundary conditions at both the shroud penetration points. It is conservative to assume hinged boundary conditions at both the shroud penetration points. All of the load combination cases were then rerun with this modified boundary condition. The collar attachment weld is a non-flux type weld and, therefore, only the primary membrane and bending stresses are of concern at this location. Also, the shear forces at this weld need not be considered since they are reacted by the core spray piping bearing against the surface of the hole in the shroud at the penetration.

The maximum axial force was calculated as 830 lbs corresponding to the faulted load combination that includes, among others, the pressure, dead weight, LOCA (double-ended guillotine break) and SSE loadings. Note that this axial force magnitude excludes the axial force due to internal pressure during core spray injection as the collar does not experience this internal pressure. Dividing the axial load carrying capability of 4816 lbs by 830 lbs gives a safety factor of 5.8 compared to the required safety factor of 1.4 for the emergency/faulted conditions.

As discussed in the attached Appendix, seismic anchor displacements based on core shroud motion are included in the analysis along with differential thermal displacements. The anchor displacement values used in the faulted condition analysis included also the shroud vertical displacement during the combined SSE plus steam line break event. The anchor displacements are maximum possible values based on the assumption that the core shroud displaces sufficiently to allow the upper bumpers for the core shroud repair to contact the reactor vessel.

Fundamental frequency of the annulus core spray piping with the hinged boundary condition assumed at the collar welds, was also determined. The objective was to evaluate if any change in the fundamental frequency would pose any FIV concerns. The fundamental frequency of the original model was 24.6 Hertz. With the modified boundary condition, the fundamental frequency decreased slightly to a value of 23.4 Hertz. It was judged that this small change in fundamental frequency would not pose any FIV concerns. Section 5 provides a detailed evaluation of potential

FIV stresses and comparison with the allowable values assuming that the collar weld has completely failed. The three cases (one assuming a hinge, second assuming full moment load carrying capability and the last one assuming a complete failure of the weld) envelop the intermediate case where the collar weld has some moment carrying capability. Table 2a through 2c show the boundary conditions used at the support points. The locations A, B, etc. are shown in Figure 5. Note that the load case assuming complete failure of the weld includes consideration of the same loading cases as the fixed and hinged boundary condition analyses plus the stresses resulting from the maximum postulated displacement at the assumed free end of the core spray piping.

#### 4. INSTALLATION TOLERANCES

The preceding structural evaluation concluded that even though the collar weld may act like a hinge it would not tear off under axial loading during next cycle of operation. This section considers the unlikely scenario in which the collar weld has completely failed and evaluates the likelihood of the section of the piping near the collar rattling under flow induced forces during normal plant operation. A key parameter in this evaluation is the potential clearance between the sparger T-box and the inside surface of the shroud.

A review of the VY core spray sparger and shroud drawings indicated that the shroud ID equals or exceeds by a maximum of 1/4 inch the expected formed sparger OD. It is expected that the sparger will tend to be tight against the shroud ID at the center of the formed sparger pipe, i.e., at the sparger T-box. The shroud drawing specifies graphically (depiction) that the sparger pipe OD should be line-on-line with the shroud ID. The sparger pipe support brackets are also shown in contact with the sparger pipe, thus the fabricator should have trimmed the brackets to fit as close to the pipe as possible. Weld shrinkage from welding the brackets would further pull the pipe towards the shroud ID. Finally the important control dimension for sparger installation is the 168.25 minimum sparger ID specified on the shroud drawing; functionally it is necessary to retain this ID for top guide removability. It is expected that the fabricator would probably have jacked the sparger pipe from the opposite side of the shroud to optimize his chance of meeting the 168.25 minimum.

Based on the preceding considerations, it is expected that the installed VY sparger pipe OD will be in contact with the shroud ID or nearly so, especially at the sparger T-box. Based on this it can be concluded that even if the collar weld were to completely fail, the core spray piping is not very likely to displace back and forth (rattle) such that FIV may be a concern.

## 5. FIV EVALUATION ASSUMING COMPLETE FAILURE OF COLLAR WELD

The discussion in the preceding Section indicates that if the collar weld is assumed to have completely failed (i.e., zero remaining ligament), the pipe in the shroud hole could potentially move 1/4 inch in the vessel radial direction. A similar review of the diametral clearance at the shroud hole indicated that the pipe can also move 0.028 inch in the lateral direction. Thus, if the collar weld were to completely fail, the pipe at that location can potentially move 1/4 inch in the vessel radial direction and 0.028 inch in the horizontal (tangential to shroud surface) and vertical directions. A conservative approach was used to calculate the FIV stresses as described next.

Figure 5 shows the finite element model of the core spray piping system with the boundary conditions indicated therein for this analysis. The three displacement load cases (0.25 inch in the radial direction, 0.028 inch in the horizontal and vertical directions) were first run. The resulting moments from the three load cases were combined by the absolute sum method and the peak stress range at each of the weld was calculated using the appropriate stress concentration factor ( $C_2K_2$ ). The stress concentration factor values used were 4.2 at the fillet weld (e.g., at the vertical slip joint) and 1.8 at the groove welds. The maximum value of the calculated alternating stress (one-half of the peak stress range) was 1398 psi. Obviously, this value is considerably less than the threshold value of 10000 psi. Based on this it is concluded that even if the collar weld is to completely fail and the core spray pipe could move the magnitude permitted by the clearances, it would not pose FIV concerns.

A primary plus secondary stress evaluation showed that even when the FIV stresses are added to the other load case stresses, the largest stress range is still less than the allowable value of  $3S_m$ .

## 6. EVALUATION ASSUMING INDICATIONS IN SHROUD

The nominal thickness of the shroud at this location is 1.75 inches. These indications are expected to be shallow (typically, less than 0.35 inch) based on field experience related to shroud cracks at sparger brackets. A bounding crack growth rate of  $5 \times 10^{-5}$  in/hr has been used in the shroud integrity evaluations. This rate implies a crack growth of 0.6 inch for 18-month cycle of operation (~12000 hrs). This would mean a predicted crack depth of less than one inch. Thus, if these indications are assumed to be in the shroud, they are not

expected to grow through the shroud wall during the next cycle of operation. Furthermore, even if it assumed that these indications become through-wall, the shroud flaw tolerance at this location is in excess of 100 inches.

Based on the preceding discussion it is concluded that shroud structural margins will be maintained if the indications are assumed on the shroud side.

## 7. SUMMARY & CONCLUSIONS

An evaluation has been performed for two limiting assumptions: (1) the indications are located in the collar, and (2) the indications are located in the shroud. The first assumption is more limiting since cracking in the collar (unlike that in the shroud wall) is likely to be through thickness. The result of this evaluation shows that even for the most limiting assumption of cracking in the thermal sleeve collar and using the previously NRC accepted conservative flaw growth rate of  $5 \times 10^{-5}$  in/hr, the structural margin requirements are met. Additionally, the leakage from the collar is not a concern because (1) the core spray injection flow is not affected, (2) any leakage of core flow would be very small due to the tight tolerances between the piping and the core shroud at the penetration location. Adequate structural margin is also maintained if the indications are located in the shroud.

Three structural load cases were evaluated. These cases were selected to envelop all possible postulated failure modes of the collar. The three bounding cases are: (1) the collar weld intact and capable of withstanding moment and translational loads, (2) the collar weld partially failed and capable of withstanding translational loads only and (3) the collar weld completely failed, in which case the core spray annulus piping is capable of displacing up to 1/4 inch axially and up to 0.028 inches vertically and horizontally. These displacements are limited by clearances between the core spray piping, sparger and core shroud.

An FIV evaluation assuming that the collar weld has completely failed and that the core spray pipe could move the magnitude permitted by the clearances, concluded that the highest alternating stress amplitude is still well below the threshold value of 10000 psi.

For all the load cases analyzed the stresses in the core spray system annulus piping are within acceptable limits.

It is concluded that the structural integrity of the core spray piping collar will be maintained and the indications are acceptable for continued operation during the next fuel cycle without repair.

## 8. REFERENCES

- [1] "BWR Core Spray Internals Inspection and Flaw Evaluation Guidelines,"  
Prepared for the BWRVIP, Report No. GE-NE-B13-01805-21, June 1996.
- [2] "Core Spray Flaw Evaluation for Vermont Yankee," GE Report No. GE-NE-523-  
B13-01805-66, Rev. 0, September 1996.



**Table 1 Indication Geometry and Ligament Calculation**

Indication No.	Indication Start (°)	Indication Finish (°)	Indication Length (°)	Length (in.)	As-Found Ligament Length (in)	Ligament Length After One Cycle (in.) <sup>1</sup>
1	15.32	24.34	9.02	0.51		
					1.81	0.61
2	56.80	94.68	37.88	2.12		
					0.80	0.00
3	109.11	154.20	45.09	2.53		
					0.90	0.00
4	170.43	251.23	80.80	4.52		
					1.00	0.00
5	269.27	332.39	63.12	3.53		
					0.50	0.00
6	341.41	4.86	23.45	1.31		
					0.58	0.00

Note (1): Based on a crack growth rate of  $5.0 \times 10^{-5}$  in/hr. For 18 month fuel cycle (approx. 12000 hours of hot operation), this crack growth rate is equivalent to a growth of 0.6 inch at each end of an indication or a reduction of 1.2 inch in the ligament between the two indications.

**Table 2a Displacement/Rotation Boundary Conditions at Various Support Points  
for Uncracked Collar Weld case**

Location	Displacement			Rotation		
	x	y	z	x	y	z
A	fixed	fixed	fixed	fixed	fixed	fixed
B <sup>1</sup>	fixed	free	free	free	free	free
C	fixed	fixed	fixed	fixed	fixed	fixed
D <sup>1</sup>	fixed	free	free	free	free	free
E	fixed	fixed	fixed	fixed	fixed	fixed

Note 1: At this support, x is radial to vessel centerline, y is circumferential and z is vertical

**Table 2b Displacement/Rotation Boundary Conditions at Various Support Points  
for hinged Collar Weld case**

Location	Displacement			Rotation		
	x	y	z	x	y	z
A	fixed	fixed	fixed	free	free	free
B <sup>1</sup>	fixed	free	free	free	free	free
C	fixed	fixed	fixed	fixed	fixed	fixed
D <sup>1</sup>	fixed	free	free	free	free	free
E	fixed	fixed	fixed	fixed	fixed	fixed

Note 1: At this support, x is radial to vessel centerline, y is circumferential and z is vertical



**Table 2c Displacement/Rotation Boundary Conditions at Various Support Points  
for Fully Cracked Collar Weld case**

Location	Displacement			Rotation		
	x	y	z	x	y	z
A	specified <sup>2</sup>	specified <sup>2</sup>	specified <sup>2</sup>	free	free	free
B <sup>1</sup>	fixed	free	free	free	free	free
C	fixed	fixed	fixed	fixed	fixed	fixed
D <sup>1</sup>	fixed	free	free	free	free	free
E	fixed	fixed	fixed	fixed	fixed	fixed

- Notes: (1) At this support, x is radial to vessel centerline, y is circumferential and z is vertical.  
 (2) For FIV Stress calculation, three load cases were run for each of the x-, y-, z-  
 displacements and the stresses added absolutely.

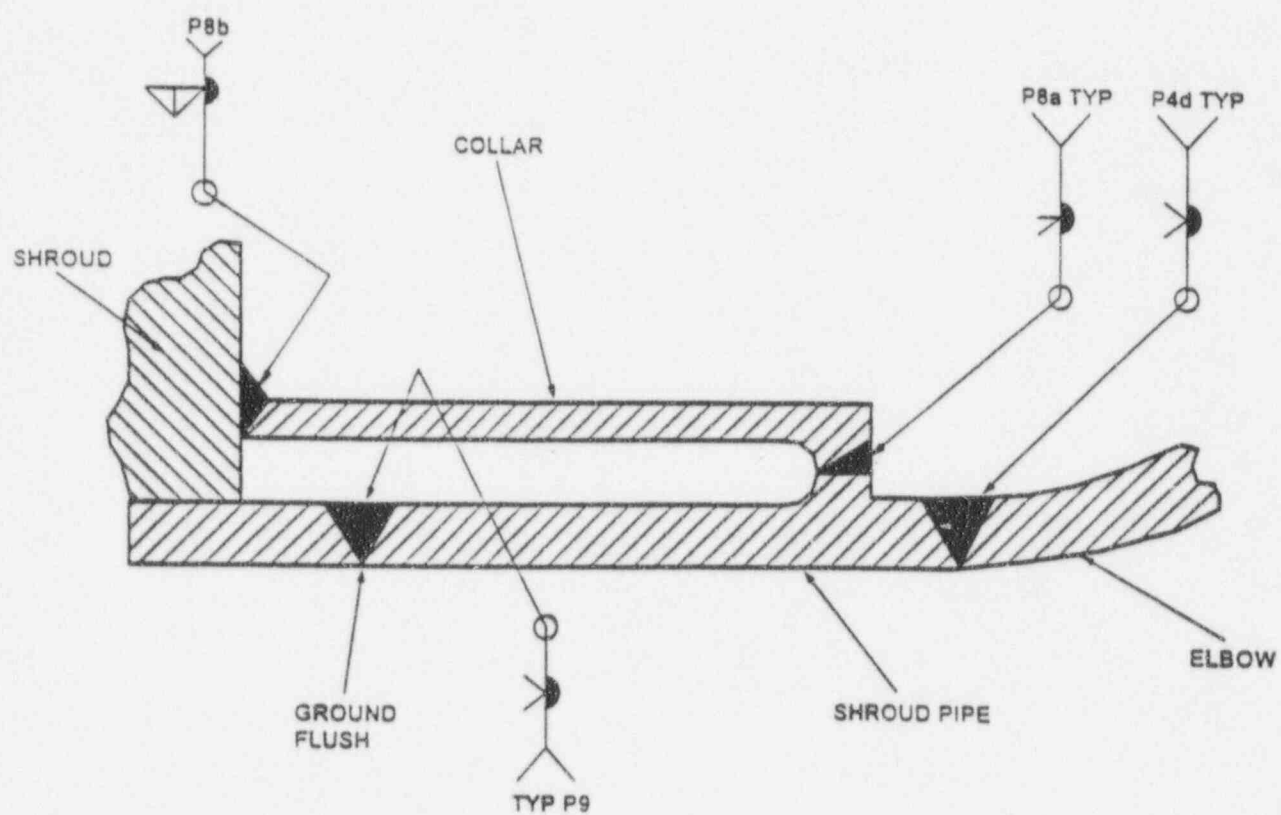


Figure 1 Attachment Weld Configuration (Reference 1)

Figure 2 Reportable Indications at Collar Weld

<b>GE Inspection Services</b>		<b>CORE SPRAY ULTRASONIC EXAMINATION</b> <b>INDICATION DATA SHEET</b> <b>(AUTOMATED with Smart 2000)</b>	
SITE: VERMONT YANKEE	PROCEDURE NO.: UT-VYM-S11V0	WELD ID: 3P8B	
UNIT: 1	REVISION / FRR NO.: 0	REPORT NO.: 104-1F8D9-RPT1	
PROJECT NO.: 1F8D9		DATA SHEET NO.: 3P8B-15	

**WELD IDENTIFICATION: 3P8B**

CONFIGURATION: Collar to Shroud  
 INDICATION SIDE: Shroud  
 DIAMETER: 8.375" (Collar)  
 CIRCUMFERENCE: 20.03"  
 INCHES/DEGREE: 0.56"  
 DEGREE/INCH: 17.97"  
 INDICATION %: 72.49%

INDICATION NUMBER	INDICATION START*	INDICATION STOP*	INDICATION LENGTH*	INDICATION LENGTH INCHES	LENGTH SIZING TRANSDUCER
1	15.32"	24.34"	9.02"	0.51"	70°
2	58.80"	94.88"	37.88"	2.12"	70°
3	109.11"	154.20"	45.09"	2.53"	70°
4	170.43"	251.23"	80.80"	4.52"	70°
5	289.27"	332.39"	43.12"	3.53"	70°
6	341.41"	4.68"	23.45"	1.31"	70°
<b>Total</b>			<b>259.36"</b>	<b>14.62"</b>	

70° TRANSDUCER  
A AND C SCAN PRESENTATIONS

70° TRANSDUCER  
A AND C SCAN PRESENTATIONS

*Michael Ball II* 9/23/96  
 EXAMINER LEVEL DATE

*John Smith* 9/24/96  
 GE REVIEWED BY LEVEL DATE

*Carl Jensen III* 10/1/96  
 UTILITY REVIEW DATE

PAGE: 1 OF: 2

FORM UT-1, 81

### Figure 2 Reportable Indications at Collar Weld (Cont'd)

GE Inspection Services

CORE SPRAY ULTRASONIC EXAMINATION  
DATA SHEET  
(AUTOMATED with Smart 2000)

SITE: VERMONT YANKEE

UNIT: 1

PROJECT NO.: 1F8D9

PROCEDURE NO.: UT-VYM-511VQ

REVISION / FRR NO.: 0

REPORT NO.: 104-1F8D9-RPT1

DATA SHEET NO.: 3P88

CALIBRATION SHEET NO.: 1.3.5.7

Weld ID: 3P88 Azimuth: 193° Component: COLLAR FLOW → SHROUD

Exam Surface: COLLAR Diameter: 6.375" Circumference: 20.03" Degrees/Inch: 18.00°

Scan size "X": 1.20" Scan size "Y": .360" File Name: 3P888

REMARKS: SIX (6) REPORTABLE INDICATIONS. SEE INDICATION DATA SHEET FOR INDICATION PARAMETERS.

Examination  
Results:

0°-180°  
60° Reportable  
Indications

☒ Yes ☐ No

180°-360°  
60° Reportable  
Indications

☒ Yes ☐ No

0°-180°  
70° Reportable  
Indications

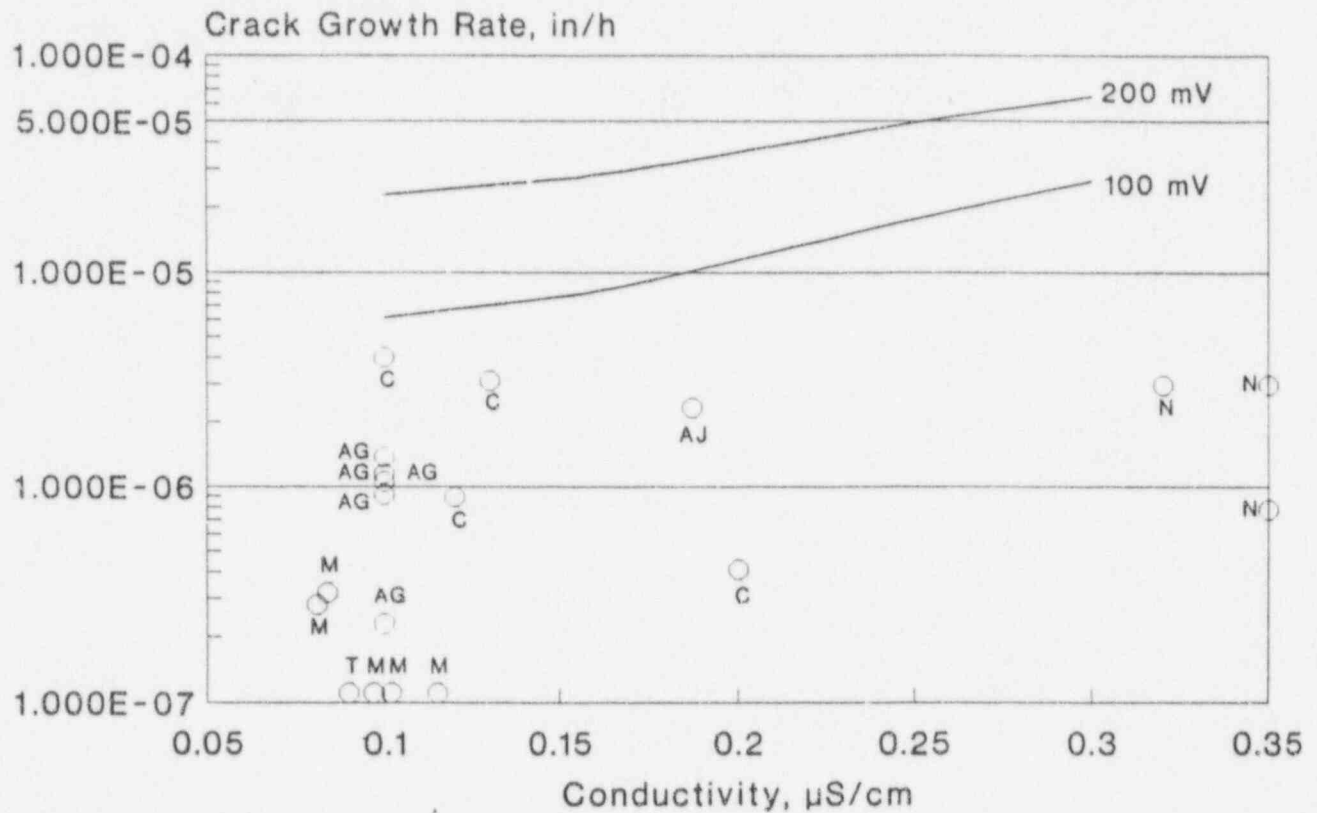
☒ Yes ☐ No

180°-360°  
70° Reportable  
Indications

☒ Yes ☐ No

FORM UT 11-91

## Effect of Conductivity on Sensitized 304 Crack Growth Rate

PLEDGE: 20 ksi $\sqrt{\text{in}}$ , 15 C/cm<sup>2</sup>CAV: 20-25 ksi $\sqrt{\text{in}}$ , 13 C/cm<sup>2</sup>, 100-160 mV

EPR20CGX

Figure 3 PLEDGE Model Crack Growth Predictions Versus Conductivity

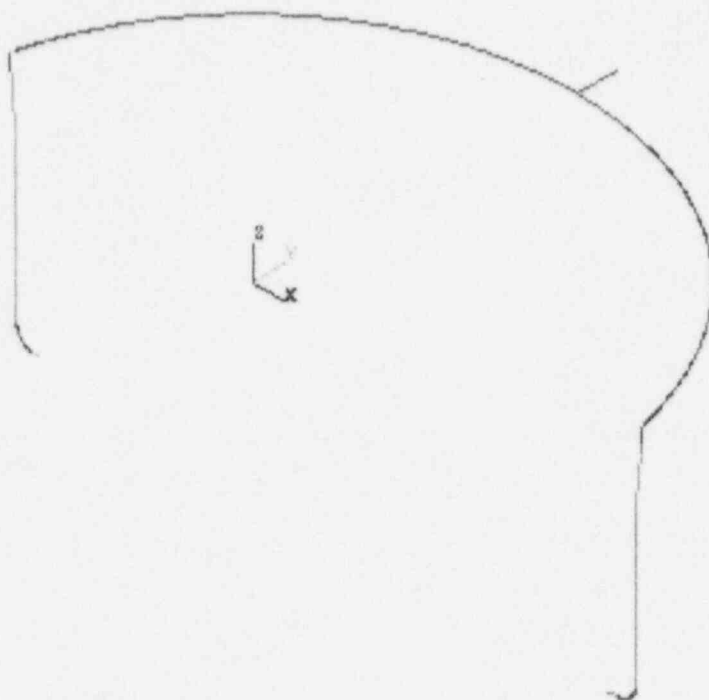


**Figure 4** ANSYS Model of the Vermont Yankee Core Spray Line

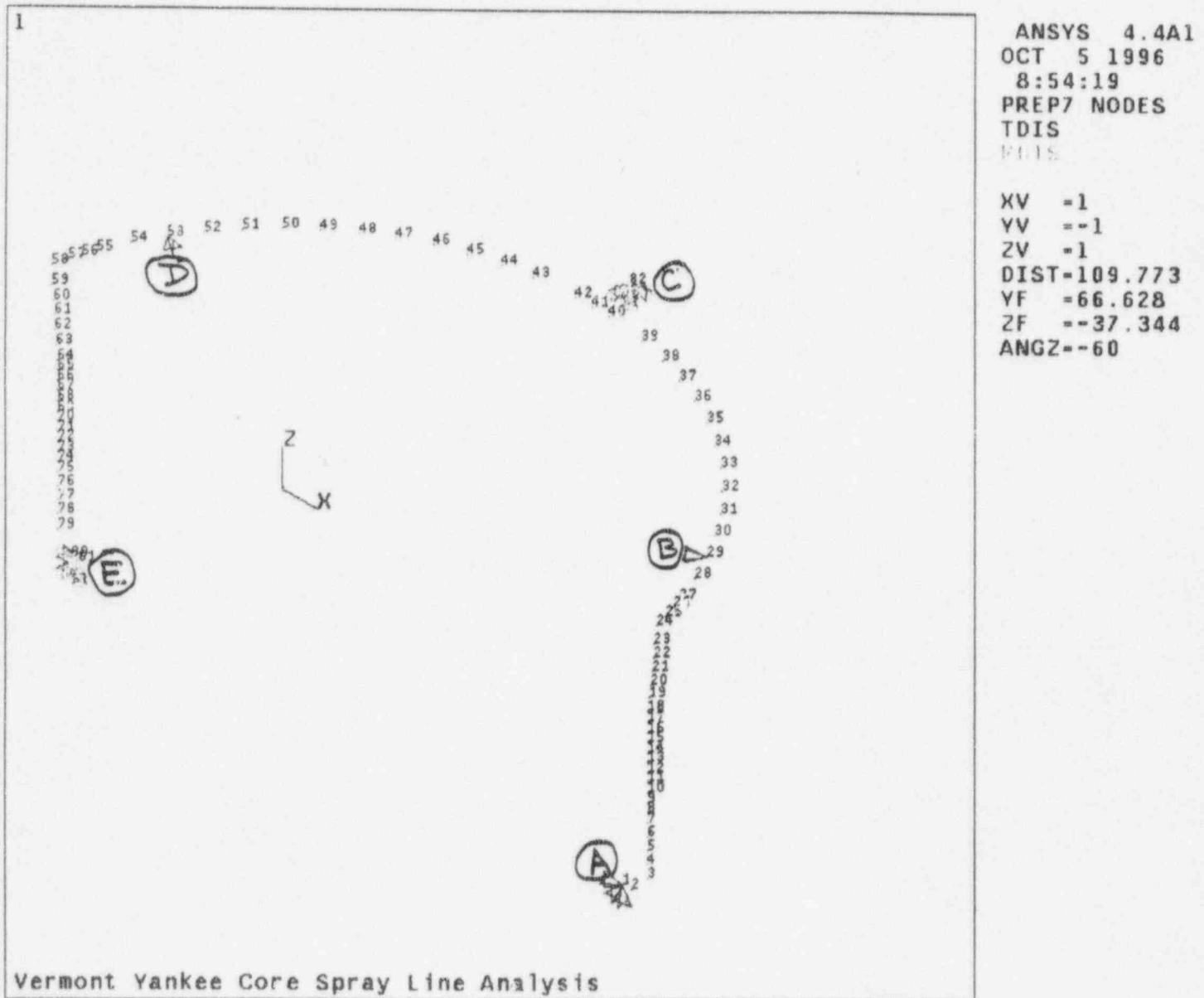


Figure 5 ANSYS Model with FIV Evaluation Boundary Conditions Shown

## APPENDIX

### FLAW TOLERANCE EVALUATION REPORT





*GE Nuclear Energy*

---

TECHNICAL MODIFICATIONS SERVICES

GE-NE-523-B13-01805-66, Rev.0

September 1996

**CORE SPRAY  
FLAW EVALUATION  
FOR  
VERMONT YANKEE**

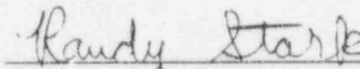
**Prepared by**

**GE Nuclear Energy  
175 Curtner Avenue  
San Jose, CA 95125**


## CORE SPRAY FLAW EVALUATION FOR VERMONT YANKEE

September 1996

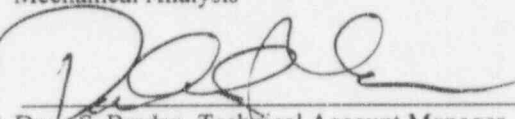
Prepared by:

  
Randy Stark, Engineer  
Mechanical Analysis

Verified by:

  
Har Mehta, Principal Engineer  
Mechanical Analysis

Approved by:

  
Dave S. Braden, Technical Account Manager  
Engineering & Licensing Consulting Services

**TABLE OF CONTENTS**

<b>1. INTRODUCTION</b>	<b>3</b>
<b>2. METHODS</b>	<b>3</b>
<b>3. ASSUMPTIONS</b>	<b>4</b>
<b>4. DESIGN INPUTS</b>	<b>4</b>
4.1. Deadweight	5
4.2. Seismic Inertia	5
4.3. Seismic Anchor Displacement	6
4.4. Fluid Drag	6
4.5. Core Spray Injection	7
4.6. Thermal loads	7
<b>5. LOAD COMBINATIONS &amp; STRESS LEVELS</b>	<b>9</b>
5.1. Load Combinations	9
5.2. Calculated Stress Levels	10
<b>6. FRACTURE MECHANICS EVALUATION</b>	<b>11</b>
6.1. Limit Load Methodology	12
6.2. Allowable Flow Length Calculation	14
6.3. Crack Growth Evaluation	16
<b>7. LEAKAGE EVALUATION</b>	<b>17</b>
7.1. Leak Rate Calculation Methodology	17
7.2. Overall Leak Rate Calculation	18
<b>8. SUMMARY &amp; CONCLUSIONS</b>	<b>18</b>
<b>9. REFERENCES</b>	<b>19</b>

## 1. INTRODUCTION

Cracking in the core spray line internal piping at several Boiling Water Reactor (BWR) plants has been recently observed. Cracking is believed to be intergranular stress corrosion cracking (IGSCC) typically in the vicinity of circumferential welds. In addition, there have been cases of cracking at creviced areas. The availability of a flaw evaluation handbook prior to actual inspection of the piping can help reduce any potential outage delay in order to disposition cracking, if any.

The objective of this report is to document the results of the flaw evaluation of the core spray internal piping (including core spray line and sparger) at the Vermont Yankee Nuclear Plant. The outcome of flaw evaluation is a set of allowable flaw lengths at key locations in the core spray internal piping system. The evaluation also includes leak rate calculations for postulated through-wall indications which can be used in an evaluation to determine if the conclusions predicted by current LOCA analyses remain valid with the postulated leakage. The overall package constitutes a flaw handbook that could be used to disposition any indications that may be detected during the inspection of core spray internal piping.

## 2. METHODS

This section presents the methodology and procedure used in performing the core spray piping analysis. Following are the steps used in the analysis.

1. Create a finite element analysis of the core spray line and sparger using the ANSYS (Reference 1) computer program. Determine the membrane and bending stresses resulting from the loadings identified in Section 4.
2. Determine the applied stresses at several key locations in the piping system and use the limit load methods of Paragraph IWB-3640, Section XI, ASME Code (see References 2 and 3) as a guide to determine the allowable flaw lengths. The rules of 1989 Edition of Section XI are used as a guide in determining the allowable flaw lengths.
3. Perform leak rate evaluations corresponding to the allowable flaw sizes (end-of-cycle).

### 3. ASSUMPTIONS

This section describes the assumptions made in the methodology of the analysis.

1. The piping system geometry is as described in the referenced drawings (Reference 4). The dimensional tolerances specified on the reference drawings are such that any variations within those values will have insignificant impact on the calculated stress values. It was also judged that any deviations between the as-built geometry and the geometry indicated in the reference drawings would not be significant in terms of stress analysis and the allowable flaw calculations.
2. The seismic inertia loads and anchor displacements were provided by Vermont Yankee.
3. Any other assumptions are stated in the body of the report.

### 4. DESIGN INPUTS

The internal core spray piping is 5-inch Schedule 40 and the material is Type 304 stainless steel. Figure 1 shows a schematic of one of the loops of the internal core spray lines. For the convenience of identification, the welds in Figure 1 have been numbered from A through L. A finite element model consisting of one loop of the internal core spray piping was developed to determine the stresses from various design loads. Figure 2 shows a line plot of the finite element model.

The internal core spray sparger was also modeled. The sparger piping is 3-inch Schedule 40, Type 304 stainless steel. Figure 3 shows a line plot of the finite element model.

The design inputs in this evaluation consisted of: (1) the geometry of the internal core spray line and sparger, and (2) the applied loads. The geometry of the internal core spray line and sparger were obtained from the drawings listed in Reference 4. The applied loads on the core spray line consist of the following: deadweight, seismic inertia, seismic anchor displacements, fluid drag, loads due to flow initiation and thermal (and internal pressure) anchor displacements. The applied loads on the core spray sparger consist of the following: deadweight, seismic inertia, and loads due to flow initiation. Each of these loads are briefly discussed next.

#### 4.1. Deadweight

The deadweight loading consists of the weight of the core spray pipe and the weight of the entrapped water. For the core spray line, the metal weight was determined as 14.6 lb/ft and the weight of the entrapped water as 8.7 lb/ft (Reference 5). For the core spray sparger, the metal weight was determined as 7.6 lb/ft and the weight of the entrapped water as 3.2 lb/ft (Reference 5). The weight of the sparger nozzles was determined to be approximately 3 lb/ft. The stresses for this loading were calculated by applying a 1.0g vertical acceleration in the finite element model of the core spray system. For flaw evaluation purposes, the stress from this loading is treated as a primary stress, and the load case designation is:

Deadweight: DW

#### 4.2. Seismic Inertia

The seismic inertia loading consists of horizontal and vertical inertia forces acting on the entire core spray line due to seismic excitation of the RPV and the core shroud. The locations where the seismic excitation is imparted to the core spray line are the vessel nozzle, the support brackets and the points where it is attached to the shroud. Likewise, the locations where the seismic excitation is imparted to the sparger are the support brackets and the tee section where it is attached to the shroud.

The following equivalent static acceleration values were used :

$$\text{OBEX} = \text{OBEZ} = 1.18g$$

$$\text{SSEX} = \text{SSEZ} = 1.5g$$

Note that the above OBE acceleration values were obtained by conservatively taking 0.85 times the SSE values. A comparison of the SSE and OBE acceleration values in Reference 6 showed the 0.85 factor to be a bounding value.

The vertical OBE acceleration value was 5.1g and the vertical SSE acceleration was 6.0g. For the purpose of specifying load combinations, the following designations are used:

Operating Basis Earthquake Inertia - X Direction: OBEIX  
Operating Basis Earthquake Inertia - Z Direction: OBEIZ  
Operating Basis Earthquake Inertia Vertical - Y Direction: OBEIY  
Safe Shutdown (or design Basis) Earthquake Inertia - X Direction: SSEIX  
Safe Shutdown (or design Basis) Earthquake Inertia - Z Direction: SSEIZ  
Safe Shutdown (or design Basis) Earthquake Inertia - Y (Vertical) Direction: SSEIY

For the flaw evaluation purposes, the stresses from the seismic inertia loading are treated as primary stresses.

#### ***4.3. Seismic Anchor Displacement***

Seismic anchor displacements are applied to the attachment points of the core spray lines at the RPV and the shroud. The following OBE condition anchor motions were obtained from seismic analysis reports (Reference 9):

OBE Displacement = 0.15 inches  
SSE Displacement = 0.177 inches

For flaw evaluation purposes, the stresses from the seismic anchor displacement loading are treated as secondary. The load case designations used are the following:

Operating Basis Earthquake Displacement - X Direction: OBEDX  
Operating Basis Earthquake Displacement - Z Direction: OBEDZ  
Design Basis Earthquake Displacement - X Direction: SEDX  
Design Basis Earthquake Displacement - Z Direction: SEDZ

#### ***4.4. Fluid Drag***

The drag loads consist of the forces resulting from the fluid flow past the core spray line. The flow in the annulus region during the normal operation exerts some downward drag force on the core spray piping. The magnitude of this loading was determined to be approximately 8.3 lb/ft assuming a conservative value of 5 ft/second for the fluid velocity in the vessel annulus region. During the upset condition, core spray operation is assumed (no feedwater flow) and, therefore, the drag loads are insignificant. During a postulated double-ended break of either the recirculation line or the main steam line, the drag loads



on the core spray line were determined to be significant (vertical loading 283 lb/ft.). This calculated loading is based on a conservatively estimated velocity in the annulus region during a LOCA event.

The drag loads are treated as primary loads for the flaw evaluation purposes and are designated as follows:

Drag Load During Normal Operation: DRG1

Drag Loads During LOCA Condition: DRG2

#### ***4.5. Core Spray Injection***

Two types of loads result when the core spray flow is initiated: internal pressure and the axial loads due to flow. During normal operation, the pressure differential between the inside and the outside of the core spray line is essentially negligible.

The internal pressure loads were calculated, using a pressure value of 82.2 psi, based on the Vermont Yankee specific process diagram (Reference 6). The membrane stress due to this internal pressure was calculated using the strength of material formulas.

The axial load due to flow, which is a function of the velocity of the flow, was calculated based on 4300 GPM flow (Reference 6).

Stresses due to water hammer loads are insignificant since the core spray inlet valve ramps open over a period of time upon system actuation. Additionally, the piping is full of water during actuation due to the presence of the vent hole on the top of the T-box. For this analysis, the core spray injection loads are treated as primary and are designated as the following:

Core Spray Injection Loads: CSIN

#### ***4.6. Thermal loads***

The two anchor points of the internal core spray line (the core spray nozzle and the brackets on the vessel at one end and the shroud attachment points at the other end)



expand vertically and horizontally at different rates due to differences in the materials' thermal expansion coefficients (low alloy steel for the vessel versus stainless steel for the shroud). Also, these displacements are expected to vary during certain transients due to the differences in temperatures between the vessel and the shroud. The loads produced by these thermal anchor displacements and thermal expansion are treated as secondary. The internal pressure in the vessel also produces vertical direction (Y) anchor motion at the nozzle and the brackets. This displacement was included along with the thermal anchor displacements. The following thermal load cases need to be considered:

Thermal displacements during Normal Steady State Operation: NOD

Thermal displacements during Loss of Feedwater Pump transient: LFWP

Thermal displacements during LOCA: LOCAD

The LOCA thermal displacements may consist of several sub-cases. One case is when the core spray is just initiated following the LOCA event. Another sub-case may be several hours following the LOCA event. The only difference between the various LOCA sub-cases would be the assumed temperatures for the vessel, the shroud, the shroud support legs and the core spray piping.

The Vermont Yankee core support structure includes shroud support legs (stilts). The stilt material is nickel-chrome-iron (Alloy 600). The RPV, shroud, and stilt lengths are used to determine the thermal displacements. The calculated values of differential thermal displacements for the various transient conditions are shown in Table 1.

Table 1. Thermal Displacements for Transient Conditions

Operat. Cond./ Transient	Temperatures (°F)			RPV Press. (psi)	Displacements (in.)		Pipe Temp (°F)
	RPV	Shroud	Stilts		Horz.	Vert.	
NOD	546	534	522	1000	0.414	-0.10	522
LFWP	500	300	300	665	0.358	0.516	300
LOCA1	546	534	522	35	0.350	-0.10	281
LOCA2	546	281	281	35	0.350	0.712	281

The Vermont Yankee vessel specification 21A1115 did not provide enough detail concerning the reactor thermal cycles. Therefore, the temperatures and pressures stated in the previous table are derived from the information contained in the RPV thermal cycle drawing of a similar plant (Reference 7).

## 5. LOAD COMBINATIONS & STRESS LEVELS

This section describes the manner in which the various loads were combined for the purpose of obtaining stress levels for flaw evaluation. The limiting stress levels in several critical areas are then summarized.

### 5.1. Load Combinations

The flaw evaluation methodology used in this analysis (similar to that in Section XI in the ASME Code), makes the distinction between two categories by specifying different safety factors. A distinction is made between the normal/upset (Level A/B) condition loads, for which the factor of safety is 2.77, and the emergency/faulted (Level C/D) condition loads, for which the safety factor is 1.39.

The following set of load combinations were considered for the evaluation of normal/upset condition for the core spray line:

- (1) DW(P) + DRG1(P) + NOD(S)
- (2) DW(P) + CSIN(P)
- (3) DW(P) + DRG1(P) + LFWP(S)
- (4) DW(P) + DRG1(P) + OBEIX(P) + OBEDX(S) + OBEIY(P) + NOD(S)
- (5) DW(P) + DRG1(P) + OBEIZ(P) + OBEDZ(S) + OBEIY(P) + NOD(S)

Note that the letter in the parenthesis indicates whether a load is primary (P) or secondary (S) as defined by the ASME Code. The set of load combinations used for the Emergency/Faulted conditions for the core spray line consist of the following:

- (1) DW(P) + DRG2(P) + SSEIX(P) + SSEIY(P) + SSEDX(S) + NOD(S)
- (2) DW(P) + DRG2(P) + SSEIZ(P) + SSEIY(P) + SSEZD(S) + NOD(S)

- (3)  $DW(P) + CSIN(P) + LOCAD(S) + SSEIX(P) + SSEIY(P) + SSADX(S)$
- (4)  $DW(P) + CSIN(P) + LOCAD(S) + SSEIZ(P) + SSEIY(P) + SSADZ(S)$

For the core spray sparger, the following set of load combinations were considered for the evaluation of normal/upset condition:

- (1)  $DW(P) + OBEIX(P) + OBEIY(P)$
- (2)  $DW(P) + OBEIZ(P) + OBEIY(P)$
- (3)  $DW(P) + CSIN(P)$

The following set of sparger load combinations were considered for the evaluation of emergency/faulted conditions:

- (1)  $DW(P) + CSIN(P) + SSEIX(P) + SSEIY(P)$
- (2)  $DW(P) + CSIN(P) + SSEIZ(P) + SSEIY(P)$

The CSIN loads included the hydraulic load at the sparger nozzles.

### 5.2. Calculated Stress Levels

The forces and moments at various nodes in the model for all of the load sources were calculated using the ANSYS finite element code (Reference 1). These forces and moments were then combined to obtain the total forces and moments for a given load combination. Thus, for each load combination and each node, a set of forces and moments were obtained. Furthermore, within each set, the forces and moments from the displacement-controlled loadings were tabulated separately for the calculation of the  $P_e$  stress. As described later, the flaw evaluation methodology uses the primary membrane ( $P_m$ ), primary bending ( $P_b$ ) and the expansion stress ( $P_e$ ).

Several weld locations were considered for the purpose of allowable flaw evaluations (see Figure 1). The calculated values of  $P_m$ ,  $P_b$  and  $P_e$  stress levels at these locations are summarized in Table 2a for the governing normal/upset and emergency/faulted condition load combinations.

For the core spray sparger, the weld location at the tee section was considered. The calculated values of  $P_m$ ,  $P_b$ , and  $P_e$  stress levels at this location is summarized in Table 2b.

Table 2a. Primary and Bending Stresses for Core Spray Line

Weld Locations (Figure 1)	Governing Oper. Cond.	Gov. Load Comb.	$P_m$ (psi)	$P_b$ (psi)	$P_e$ (psi)
A,L	Emer./Fault.	Note 1	83	3628	280
B,K	Emer./Fault.	Note 1	1204	1790	891
C,J	Emer./Fault.	Note 1	1059	1153	1553
D,I	Emer./Fault.	Note 2	485	4740	6168
E,H	Emer./Fault.	Note 2	115	5000	6566
F,G	Emer./Fault.	Note 2	150	13272	7068

Note 1: Load Comb. =  $DW(P) + DRG2(P) + SSEIX(P) + SSEIY(P) + SSEDZ(S) + NOD(S)$

Note 2: Load Comb. =  $DW(P) + DRG2(P) + SSEIX(P) + SSEIY(P) + SSEDZ(S) + NOD(S)$

Table 2b. Primary and Bending Stresses for Core Spray Sparger

Weld Locations	Governing Oper. Cond.	Gov. Load Comb.	$P_m$ (psi)	$P_b$ (psi)	$P_e$ (psi)
Tee	Norm./Upset	Note 1	661	80	0

Note 1: Load Comb. =  $DW(P) + CSIN(P)$

The stress levels in the preceding tables were used in the allowable flaw evaluations as described in the next section.

## 6. FRACTURE MECHANICS EVALUATION

The limit load methodology was used in calculating the allowable flaw lengths. This methodology is first described followed by the results of allowable flaw evaluations.

### 6.1. Limit Load Methodology

Consider a circumferential crack of length,  $l = 2R\alpha$  and constant depth,  $d$ . In order to determine the point at which limit load is achieved, it is necessary to apply the equations of equilibrium assuming that the cracked section behaves like a hinge. For this condition, the assumed stress state at the cracked section is as shown in Figure 4 where the maximum stress is the flow stress of the material,  $\sigma_f$ . Equilibrium of longitudinal forces and moments about the axis gives the following equations:

$$\beta = [(\pi - \alpha d/t) - (P_m/\sigma_f)\pi]/2 \quad (1)$$

$$P_b' = (2\sigma_f/\pi) (2 \sin \beta - d/t \sin \alpha) \quad (2)$$

Where,  $t$  = pipe thickness, inches

$\alpha$  = crack half-angle as shown in Figure 3

$\beta$  = angle that defines the location of the neutral axis

$Z$  = Weld type factor

$P_e$  = Piping expansion stress

$P_m$  = Primary membrane stress

$P_b$  = Primary bending stress

$P_b'$  = Failure bending stress

The safety factor is then incorporated as follows:

$$P_b' = Z * SF (P_m + P_b + P_e/SF) - P_m \quad (3)$$

The  $P_m$  and  $P_b$  are primary stresses.  $P_e$  is secondary stress and includes stresses from all displacement-controlled loadings such as thermal expansion, seismic anchor motion, etc. All three quantities are calculated from the analysis of applied loading. The safety factor value is 2.77 for normal/upset conditions and 1.39 for emergency/faulted conditions.

#### Z Factor

The test data considered by the ASME Code in developing the flaw evaluation procedure (Appendix C, Section XI) indicated that the welds produced by a process without using a flux had fracture toughness as good or better than the base metal. However, the flux welds had lower toughness. To account for the reduced toughness of the flux welds (as compared to non-flux welds) the Section XI procedures prescribe a penalty factor, called

a 'Z' factor. The examples of flux welds are submerged arc welds (SAW) and shielded metal arc welds (SMAW). Gas metal-arc welds (GMAW) and gas tungsten-arc welds (GTAW) are examples of non-flux welds. Figure IWB-3641-1 may be used to define the weld-base metal interface. The expressions for the value of the Z factor in Appendix C of Section XI are given as follows:

$$\begin{aligned} Z &= 1.15 [1 + 0.013(OD-4)] \text{ for SMAW} \\ &= 1.30 [1 + 0.010(OD-4)] \text{ for SAW} \end{aligned}$$

where, OD is the nominal pipe size (NPS) in inches. The procedures of Appendix C recommend the use of OD = 24 for pipe sizes less than 24-inches. This approach is very conservative and, therefore, the use of actual NPS was made in calculating the 'Z' factor. This approach is considered reasonable as recent discussions in the Section XI Code Working Group on Pipe Flaw Evaluation indicate that for small diameter pipes, such as the 5-inch diameter core spray piping, the Z-factor may be close to or less than 1.0.

Nevertheless, the allowable flaw size calculations were conducted using both the approaches (i.e., assuming a nominal core spray line diameter of 5-inches and 24-inches).

the Z-factors for the two approaches are:

$$\begin{aligned} Z_{5\text{-inch}} &= 1.15[1 + 0.013(5-4)] = 1.165 \\ Z_{24\text{-inch}} &= 1.15[1 + 0.013(24-4)] = 1.45 \end{aligned}$$

If the indication is located in the base metal or near a non-flux weld, Z is assumed as 1.0 and the  $P_e$  stresses are not used in the calculation, consistent with Appendix C guidelines. If the indication is located in or near a flux-weld, the calculation is done using both Z factors described above. For information purposes, all of the allowable flaw calculations were conducted considering both the flux and non-flux cases.

For the sparger with a nominal diameter of 3 inches, the corresponding values of A are:

$$\begin{aligned} Z_{5\text{-inch}} &= 1.15[1 + 0.013(0)] = 1.15 \\ Z_{24\text{-inch}} &= 1.15[1 + 0.013(24-4)] = 1.45 \end{aligned}$$

## 6.2. Allowable Flaw Length Calculation

The stresses from the table in the preceding section were used to determine the acceptable end-of-cycle through-wall flaw lengths. The acceptable flaw size was determined by requiring a safety factor. The flow stress was taken as  $3S_m$  ( $S_m=16.9$  ksi for Type 304 stainless steel at 550°F). As specified in Reference 2, safety factors of 2.77 for the normal/upset conditions and 1.39 for the emergency/faulted conditions, respectively, were used. Since the stress analysis considered the welds at the coupling to be intact, the allowable flaw lengths were independent of the engagement length. The calculated values of the allowable flaw lengths for the core spray line are tabulated, and shown in Table 3a. It should be noted that the regions of the smallest allowable flaw lengths, near the tee box connection (welds F and G) and the header to riser connection (welds I and D) are regions that a non-flux welding process is generally used.



Table 3a. Allowable Flaw Lengths for Core Spray Line (End-of-Cycle)

Weld Location (Figure 1)	Weld Type	Total Allowable Effective Crack w/o Crack Growth Added		Total Allowable Effective Crack with One Cycle of Crack Growth		Total Allowable Effective Crack with Two Cycles of Crack Growth	
		Angle (deg.)	Length (in.)	Angle (deg.)	Length (in.)	Angle (deg.)	Length (in.)
A,L	<i>non-flux</i>	231.53	11.24	206.81	10.04	182.09	8.84
	<i>flux, Z= 1.165</i>	222.62	10.81	197.90	9.61	173.18	8.41
	<i>flux, Z= 1.45</i>	210.89	10.24	186.17	9.04	161.45	7.84
B,K	<i>non-flux</i>	233.21	11.32	208.50	10.12	183.78	8.92
	<i>flux, Z= 1.165</i>	220.42	10.70	195.70	9.50	170.98	8.30
	<i>flux, Z= 1.45</i>	210.12	10.20	185.40	9.00	160.68	7.80
C,J	<i>non-flux</i>	244.18	11.85	219.46	10.65	194.74	9.45
	<i>flux, Z= 1.165</i>	224.82	10.91	200.10	9.71	175.39	8.51
	<i>flux, Z= 1.45</i>	214.85	10.43	190.13	9.23	165.41	8.03
I,D	<i>non-flux</i>	213.44	10.36	188.72	9.16	164.01	7.96
	<i>flux, Z= 1.165</i>	168.90	8.20	144.18	7.00	119.46	5.80
	<i>flux, Z= 1.45</i>	151.53	7.36	126.81	6.16	102.09	4.96
E,H	<i>non-flux</i>	216.10	10.49	191.38	9.29	166.66	8.09
	<i>flux, Z= 1.165</i>	168.22	8.17	143.50	6.97	118.78	5.77
	<i>flux, Z= 1.45</i>	150.44	7.30	125.72	6.10	101.00	4.90
F,G	<i>non-flux</i>	155.01	7.53	130.29	6.33	105.57	5.13
	<i>flux, Z= 1.165</i>	113.75	5.52	89.04	4.32	64.32	3.12
	<i>flux, Z= 1.45</i>	87.91	4.27	63.19	3.07	38.47	1.87

The resulting allowable crack lengths are tabulated in the last column for an end-of-cycle case, assuming a crack growth of 1.2 inches (18-month fuel cycle). The basis for the 1.2 inch crack growth is discussed in the next Subsection.

The calculated values of the allowable flaw lengths for the core spray sparger are tabulated, and shown in Table 3b.



Table 3b. Allowable Flaw Lengths for Core Spray Sparger (End-of-Cycle)

Weld Location	Weld Type	Total Allowable Effective Crack w/o Crack Growth Added		Total Allowable Effective Crack with One Cycle of Crack Growth		Total Allowable Effective Crack with Two Cycles of Crack Growth	
		Angle (deg.)	Length (in.)	Angle (deg.)	Length (in.)	Angle (deg.)	Length (in.)
Tee	<i>non-flux</i>	255.39	7.80	216.10	6.60	176.81	5.40
	<i>flux, Z= 1.15</i>	251.34	7.68	212.05	6.48	172.76	5.28
	<i>flux, Z= 1.45</i>	243.95	7.45	204.67	6.25	165.38	5.05

### 6.3. Crack Growth Evaluation

Prior crack growth analyses performed for BWR shroud indications have conservatively used a crack growth rate of  $5 \times 10^{-5}$  inch/hot hour.

The stresses induced in the core spray line are very low, as evidenced by the stress results presented in the previous section. Those stress results also conservatively include the effects of seismic and core spray injection loads, which are not typically present. Therefore, the applied stress intensity factor is low, and the corresponding crack growth rate would be significantly below the upper bound value of  $5 \times 10^{-5}$  inch/ hot hour used here.

Pre-operational testing of BWR internals has demonstrated that high cycle fatigue resulting from flow induced vibration is not a concern for the core spray piping. Additionally, low cycle fatigue caused by assumed thermal transients which could be potentially imposed by cold fluid injection through the feedwater spargers located directly above the core spray lines have been found to be insignificant. Therefore, fatigue crack propagation of indications in the core spray lines is concluded to be negligible, and is not considered to be a further contributor to the crack growth values discussed here.

Thus, a conservative crack growth rate of  $5 \times 10^{-5}$  in/ hot hr can be used in the flaw evaluations. This crack growth rate translates into a crack length increase of (8000 hrs

per year  $\times 1.5 \times 10^{-5}$ ) or 0.6 inch at each end of an indication assuming a 18-month fuel cycle. Thus, the projected length,  $l_f$ , of any indication whose current length at the time of inspection is  $l_p$ , would be  $(l_p + 0.6 \times 2)$  inches. A factor of 2 in the preceding parenthesis is to account for the growth at each end of the indication.

## 7. LEAKAGE EVALUATION

### 7.1. Leak Rate Calculation Methodology

The leakage from the core spray line into the RPV annulus could come from a number of sources such as through the 0.25 inch vent hole at the top of the T-box, through the gap between the sleeve and the nozzle ID, and through the presence of any through-wall cracks in the piping. The leakage rate through the vent hole was estimated assuming incompressible Bernoulli flow through the hole:

$$Q = CA\sqrt{2g_c\Delta P/\rho} \quad (4)$$

where,  $Q$  = Leakage

$C$  = flow coefficient (assumed to be 0.6 for an abrupt contraction as in the case of vent hole)

$A$  = area

$\rho$  = mass density of fluid

$\Delta P$  = pressure difference across the pipe/vent

A  $\Delta P$  value of 82.2 psi based on Reference 6 was used. This is the upper bound value of steady state pressure during the core spray operation for this plant.

Leak rate from the through-wall indications in the core spray line can also be estimated using the preceding equation with the value of flow coefficient,  $C$ , assumed as 1.0. A key input needed is the crack opening area,  $A$ .

The approach used in this evaluation to calculate the value of  $A$ , was to assume a conservative value of crack opening displacement,  $\delta$ , and assume the crack opening configuration to be like a rectangular slot with one side being the crack length,  $2a$ , and the other side as the crack opening displacement. A value of 0.01 inch was assumed for  $\delta$ . Linear elastic fracture mechanics calculations indicated this assumed value of  $\delta$  to be very conservative. The crack opening area is then simply:

$$A = 2a(\delta) \quad (5)$$

### **7.2. Overall Leak Rate Calculation**

The leak rate was calculated using an internal pressure of 82.2 psi. Using this value as the  $\Delta P$  and equation (4) gave a 11.9 gpm leak rate from the vent hole.

The leak rates from any indications would be a function of the detected number and lengths of the indications which will be known only after an examination of the internal core spray piping has been conducted. To facilitate this calculation after the examination results are determined, leak rate per inch of crack length is provided herein. This leak rate was calculated as 4.0 gpm per inch of crack length. It should be noted that the crack length to be used for leak rate calculation should include expected crack growth during the next operating cycle.

This leakage calculation can be used to evaluate the effect on the current SAFER/GESTR LOCA analysis, and to demonstrate that the conclusions are still applicable.

## **8. SUMMARY & CONCLUSIONS**

A flaw evaluation, consisting of stress and limit load analyses of the internal core spray piping of Vermont Yankee was performed to develop a flaw disposition handbook. Procedures similar to those in Paragraph IWB-3640, ASME Section XI, were used in determining the allowable flaw lengths. Allowable flaw lengths were calculated at seven critical locations and leak rate calculation methodology was presented. The methodology presented in this report can also be used to disposition any indications detected during the future inspections of the internal core spray line and sparger.

## 9. REFERENCES

- [1] DeSalvo, G.J., Ph.D. and Swanson, J. A., Ph.D., ANSYS Engineering Analysis System User's Manual, Revision 4.4, Swanson Analysis Systems, Inc., Houston, PA, May 1, 1989.
- [2] ASME Boiler and Pressure Vessel Code, Section XI, Rules for In-Service Inspection of Nuclear Power Plant Components, American Society of Mechanical Engineers, 1989 Edition, Paragraph IWB 364C.
- [3] Ranganath, S. and Mehta, H. S., "Engineering Methods for the Assessment of Ductile Fracture Margin in Nuclear Power Plant Piping," Elastic-Plastic Fracture: Second Symposium, Volume II - Fracture Resistance Curves and Engineering Applications, ASTM STP 803, C.F. Shih and J. P. Gudas, Eds., American Society for Testing and Materials, 1983, pp. II-309 - II-330.
- [4] Vermont Yankee Drawings: (a) Shroud Drg #5920-528, (b) Core Spray Line Drg #5920-1806, (c) Vessel Drg #5920-103, (d) Reactor Assembly Drg #5920-3773 and #5920-3774, (e) Core Spray Sparger Drg #5920-3776.
- [5] Avallone, Eugene A. and Baumeister, Theodore III, "Marks' Standard Handbook for Mechanical Engineers", Ninth Edition, McGraw-Hill, 1987.
- [6] "Vermont Yankee Nuclear Power Station - Primary Structure Seismic Analysis for Core Shroud Evaluation", GE Report No. GE-NE-523-A194-1294, Rev. 0, DRF No. B13-01750, December 1994.
- [7] "Reactor Thermal Cycles," GE Drawing No. 761E708.
- [8] Vermont Yankee FSAR, Figure 6.4.2.
- [9] Letter from H. William McCurdy of MPR to John R. Hoffman of Yankee Atomic Electric Company dated June 25, 1996, "Vermont Yankee Core Shroud Repair - Seismic Acceleration at Core Spray Piping Attachments at Shroud and Reactor Vessel", (with MPR Calculation No. 249-9502-728 Rev. 1 and three diskettes containing digitized acceleration time histories).

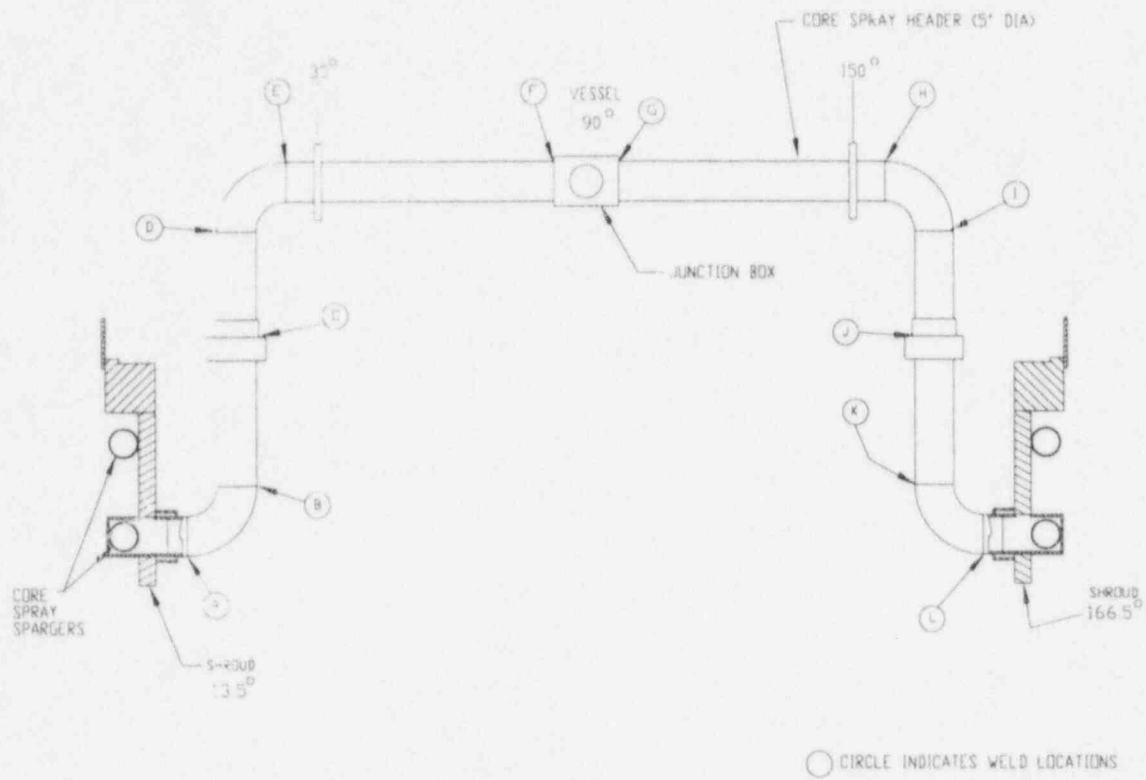


**Figure 1 Schematic of Vermont Yankee Internal Core Spray Piping Configuration**

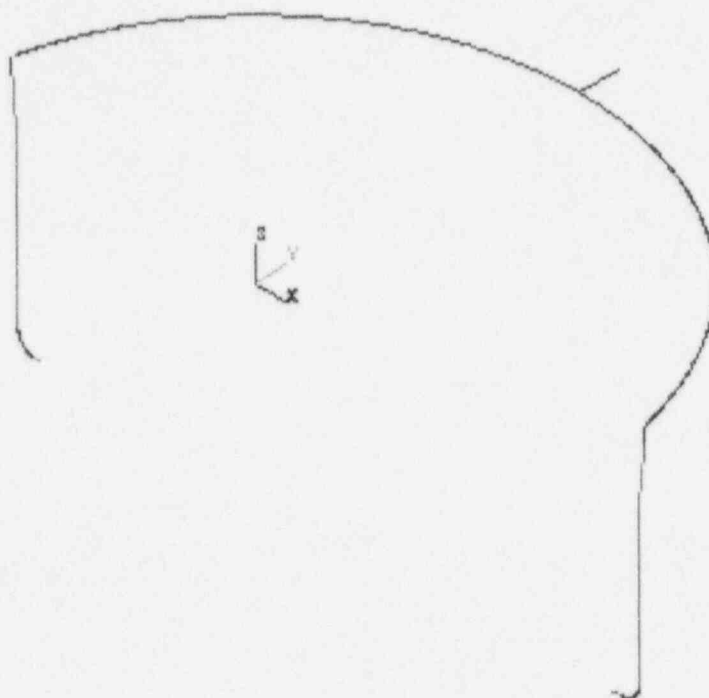


**Figure 2 ANSYS Model of the Vermont Yankee Core Spray Line**

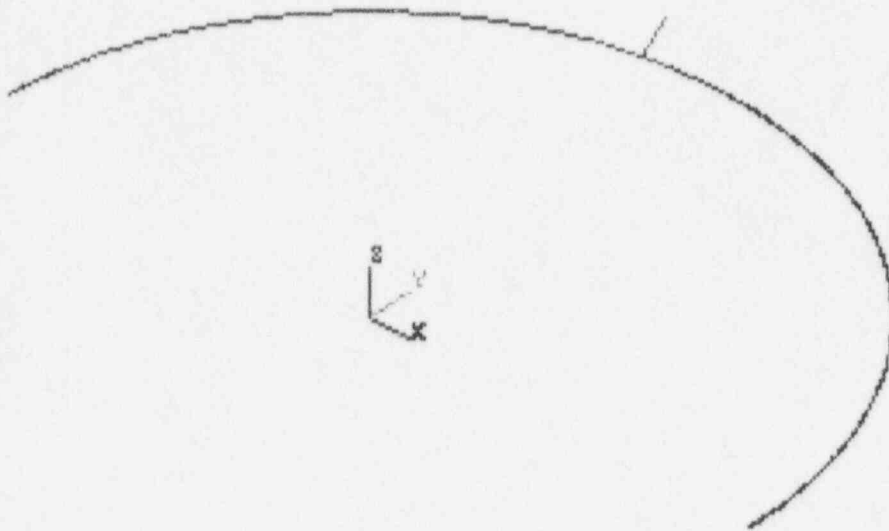


**Figure 3 ANSYS Model of the Vermont Yankee Core Spray Sparger**

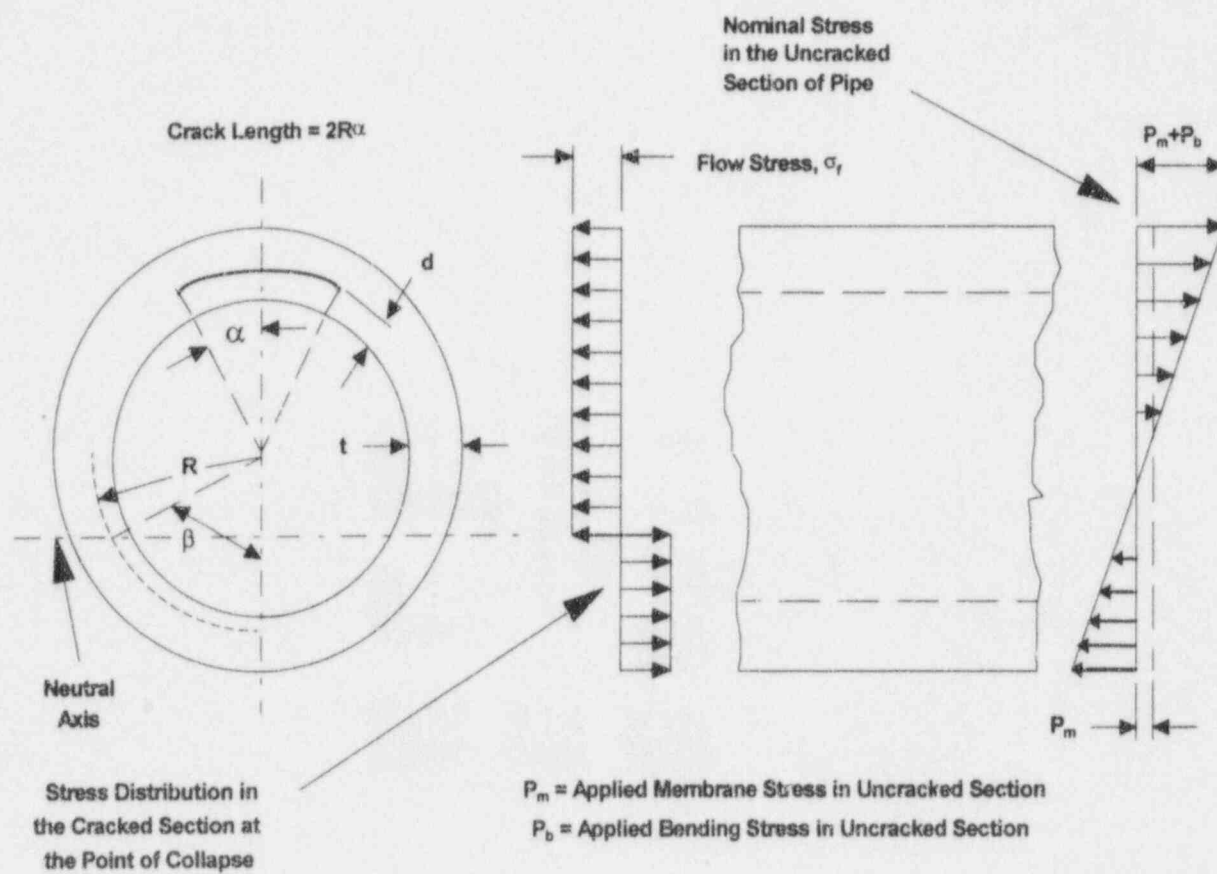


Figure 4 Stress Distribution in a Cracked Pipe at the Point of Collapse